Applied Mathematics and Nonlinear Sciences 3(2) (2018) 339–352

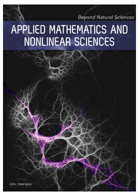

Applied Mathematics and Nonlinear Sciences

https://www.sciendo.com

Calculation of line of site periods between two artificial satellites under the action air drag

M. K. Ammar[a]†, M. R. Amin[b], M.H.M. Hassan[c]

Department of Mathematics, Faculty of Science, Helwan University, Cairo, Egypt,
E-mail: Sciencemh@yahoo.com[a,c]

Theoretical Physics, Dept. National Research Center - Giza, Egypt, E-mail: Mohammed.nrc@gmail.com[b]

Submission Info

Communicated by Elbaz I. Abouelmagd
Received 23th January 2018
Accepted 20th June 2018
Available 1st July 2018

Abstract

In a previous (herein referred to as Ammar, Amin and Hassan Paper [1]) the statement of the problem was formulated and the basic visibility function between two satellites in terms of the orbital elements and time were derived. In this paper the perturbing effect due to drag force on the visibility function were derived explicitly up to $O(e^4)$, by using Taylor's expansion for the visibility function about certain epoch. We determine the rise and set times of the satellites through the sign of the visibility function. Numerical examples were worked out for some satellites in order to check the validity of the work.

Keywords: Visibility function - line of site - Air Drag force - rise and set times.
AMS 2010 codes: 70F15

1 Introduction

Rise–set time computation through the accurate orbit estimation is very important because it plays an essential role in the pre-request information for mission analysis and on-board resources management in many general communication, scientific spacecraft and Earth observation. Also, to provide and exchange information for a wide range of military and civil applications such as communications, there is a big trend to use fast access, low cost and multifunctional small satellites. This requires accurate estimation of when the satellites disappears from the horizon (set) over a time-scale of months in some cases and when the satellite will start to be visible (rise) to a given location on the Earth or to other satellite. Therefore, we referred in Ammar and Hassan [1], to

†Corresponding author.
Email address: Medhatammar24@gmail.com

ISSN 2444-8656 doi:10.21042/AMNS.2018.2.00027

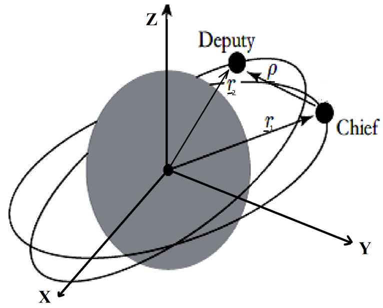

Fig. 1 Geometry of Satellites Visibility

the rise/set problem which may be defined as the process of determining the times at which a satellite rises and sets with respect to a ground location. The numerical method is the easiest solution to determine the visibility periods for the site and satellite by evaluating UK position vectors of each. It advances vectors by a small time increment, Δt,and checks visibility at each step. Computation time is a drawback to this method, especially when modeling many perturbations and processing several satellites. Escobal [2], [3] proposed a faster method to solve the rise/set problem by developing a closed-form solution for unrestricted visibility periods about an oblate Earth. He assumes infinite range, azimuth, and elevation visibility for the site. Escobal transforms the geometry for the satellite and tracking station into a single transcendental equation for time as a function of eccentric anomaly. He then uses numerical methods to find the rise and set anomalies, if they exist. Lawton [4] has developed another method to solve for satellite-satellite and satellite-ground station visibility periods for vehicles in circular or near circular orbits by approximating the visibility function, by a Fourier series. More recently, Alfano, Negron, and Moore [5] derived an analytical method to obtain rise/set times of a satellite for a ground station and includes restrictions for range, azimuth, and elevation. The algorithm uses pairs of fourth-order polynomials to construct functions that represent the restricted parameters (range, azimuth, and elevation) versus time for an oblate Earth. It can produce these functions from either uniform or arbitrarily spaced data points. The viewing times are obtained by extracting the real roots of localized quantic. Palmar [6], introduced a new method to predict the passes of satellite to a specific target on the ground which is useful for solving the satellite visibility problem. he firstly described a coarse search phase of this method including two-body motion, secular perturbation and atmospheric drag, then he described the second phase (refinement), which uses a further developed controlling equation $F(\alpha) = 0$ based on the epicycle equations.

In this work, we established a fast way for satellite-satellite visibility intervals for the rise-and-set time prediction for two satellites in terms of classical orbital elements of the two satellites and time. We have considered the secular variations of the orbital elements due to air drag force in order to determine the changes in the nodal period of satellite and the changes in the long-term prediction of maximum elevation angle. In the following description, we will introduce the formulae for satellite rise-and-set times of the two satellites. The derived visibility function provides high accuracy over a long period.

2 Visibility Analysis

In order to fully describe the position of a satellite in space at any given time, we used a set of six orbital parameters semi-major axis a, eccentricity e, inclinations of the orbit plane i, right ascension of the node Ω, the argument of perigee ω, and true anomaly f. The above parameters are shown in the Fig.1.

The visibility function, U, which describes whether these two satellites can achieve visibility were derived in Ammar and Hassan [1], Eq. 1 and in briefly it can be obtained as follows:

$$U = R_e^2\left[\left({r_1}^2 + {r_2}^2\right) - 2\left(\vec{r}_1 \cdot \vec{r}_2\right)\right] - {r_1}^2{r_2}^2 + \left(\vec{r}_1 \cdot \vec{r}_2\right)^2 \tag{1}$$

Where

$$U = \begin{cases} +ve\ ,\ Non-visibility\,case \\ 0\ ,\ rise\ or\ set \\ -ve\ ,\ direct-line\,of-sight \end{cases}$$

Referring to Fig.1, the position vectors of satellites 1, and 2 with respect to the ECI coordinate system are $\vec{r}_1$ and $\vec{r}_2$.

If the position relation between two satellites satisfies the visibility conditions, two satellites can communicate with each other over interstellar links.

3 Construction of The Visibility Function

The position vector of each satellite in the geocentric coordinate system, $\vec{r} = (x, y, z)$, can be calculated by the following formula [7],

$$\begin{pmatrix} x \\ y \\ z \end{pmatrix} = r \begin{pmatrix} \cos\Omega\cos(\omega+f) - \sin\Omega\sin(\omega+f)\cos i \\ \sin\Omega\cos(\omega+f) + \cos\Omega\sin(\omega+f)\cos i \\ \sin(\omega+f)\sin i \end{pmatrix}$$

Where r denote the distance from the earth center O to the satellite, given by:

$$r = \frac{a(1-e^2)}{1+e\cos f}$$

Forming scalar product $(\vec{r}_1 \cdot \vec{r}_2)$, keeping terms up to $O(e^4)$ only, we obtain

$$\vec{r}_1 \cdot \vec{r}_2 = x_1 x_2 + y_1 y_2 + z_1 z_2$$

For the sake of simplification of calculations, we put the coordinates of the satellite as:

$$\begin{aligned} x_1 &= r_1 \left[\sigma_1{}^2 \cos(f_1+\omega_1+\Omega_1) + \gamma_1{}^2 \cos(f_1+\omega_1-\Omega_1)\right] \\ y_1 &= r_1 \left[\sigma_1{}^2 \sin(f_1+\omega_1+\Omega_1) - \gamma_1{}^2 \sin(f_1+\omega_1-\Omega_1)\right] \\ z_1 &= 2\, r_1\, \sigma_1\, \gamma_1 \cos(f_1+\omega_1) \end{aligned} \tag{2}$$

Where $\sigma_1 = \cos(i_1/2)$ *and* $\gamma_1 = \sin(i_1/2)$, with similar expressions for the other satellite. In order to obtain the visibility function as an explicit function of time, we transform the true anomaly f, to the mean anomaly, M, using the following transformation formulas Brouwer [7] up to $O(e^4)$,

$$\begin{aligned} r_1 = a_1 \Big[&\left(1+\tfrac{1}{2}e_1^2\right) + \left(-e_1+\tfrac{3}{8}e_1^3\right)\cos M_1 + \left(-\tfrac{1}{2}e_1^2+\tfrac{1}{3}e_1^4\right)\cos 2M_1 \\ &-\tfrac{3}{8}e_1^3\cos 3M_1 - \tfrac{1}{3}e_1^4\cos 4M_1\Big] \end{aligned} \tag{3}$$

$$\begin{aligned} r_1\cos f_1 = a_1 \Big[&-\tfrac{3}{2}e + \left(1-\tfrac{3}{8}e_1^2+\tfrac{5}{192}e_1^4\right)\cos M_1 - \left(\tfrac{1}{2}e_1+\tfrac{1}{3}e_1^3\right)\cos 2M_1 \\ &+\left(-\tfrac{1}{2}e_1^2+\tfrac{1}{3}e_1^4\right)\cos 2M_1 + \left(\tfrac{3}{8}e_1^2-\tfrac{45}{128}e_1^3\right)\cos 3M_1 + \tfrac{1}{3}e_1^3\cos 4M_1\Big] \end{aligned} \tag{4}$$

$$\begin{aligned} r_1\sin f_1 = a_1 \Big[&\left(1-\tfrac{5}{8}e_1^2-\tfrac{11}{192}e_1^4\right)\sin M_1 + \left(\tfrac{1}{2}e_1-\tfrac{5}{12}e_1^3\right)\sin 2M_1 \\ &+\left(\tfrac{3}{8}e_1^2-\tfrac{51}{128}e_1^4\right)\sin 3M_1 + \tfrac{1}{3}e_1^3\sin 4M_1\Big] \end{aligned} \tag{5}$$

With similar expressions for the other satellite. Substituting Eqs. (3-5) into Eq. (2), and keeping terms up to $O(e^4)$, we obtain the visibility function [Ammar and Hassan [1]]:

4 The Effect of Drag

The acceleration due to air drag has the general form [8]

$$\vec{F}_D = -\frac{1}{2m} C_D A_s \rho_{air} V^2 \ \underline{\hat{V}}$$

Where, m is the satellite mass, C_D is the aerodynamic drag coefficient, A_s is the average cross-sectional area of the satellite, ρ_{air} is the air density and V is the magnitude of the satellite velocity relative to the atmosphere, and is the unit vector in the satellite velocity direction.

Since the drag force is non-conservative, so we will use Lagrange's planetary equations in Gaussian form Roy [9] expressed in the R S W - coordinate system, i.e. in the directions of the radial, transverse and orthogonal respectively, shown in Fig. 2.

Also, since the drag force in the opposite direction of the velocity vector, then we can express the drag acceleration components in the form:

$$\vec{F}_D = (F_R, F_S, 0) = (-|F_D| \cos\varphi, -|F_D| \sin\varphi \ , 0)$$

Where φ is the flight path angle.

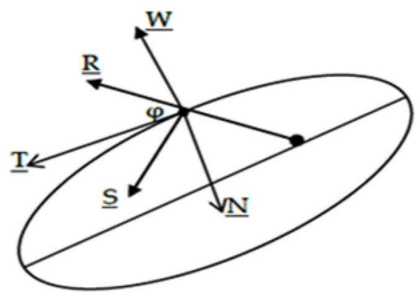

Fig. 2 The relation between RSW and TNW-Coordinate systems

Expressing *sinφ* and *cosφ* in terms of the true anomaly *f*, by using the well-known relations:

$$\cos\varphi = \frac{1+e\cos f}{\sqrt{1+e\cos f+e^2}}, \quad \sin\varphi = \frac{e\sin f}{\sqrt{1+e\cos f+e^2}}$$

We can write the rate of change of the osculating elements of the satellite in the RSW- Coordinate system in the form :

$$\frac{da}{dt} = \frac{2}{n\sqrt{1-e^2}} [(e\sin f) F_R + (1+e\cos f) F_S]$$

$$\frac{de}{dt} = \frac{\sqrt{1-e^2}}{na} \left[(\sin f) \ F_R + \frac{(e+2\cos f + e\cos^2 f)}{(1+e\cos f)} F_S \right]$$

$$\frac{d\omega}{dt} = \frac{\sqrt{1-e^2}}{nae} \left[-(\cos f) F_R + \frac{(2+e\cos f)}{(1+e\cos f)} (\sin f) F_S \right]$$

$$\frac{dM}{dt} = n + \frac{(1-e^2)}{nae} \left[\left(\sin f - \frac{2e}{(1+e\cos f)} \right) F_R - \frac{(2+e\cos f)}{(1+e\cos f)} (\sin f) F_S \right]$$

Since the drag force oppose the velocity vector. Hence, we need to find the drag components in the TNW - coordinate system, where T- axis aligned along the tangent (velocity vector), N - axis normal to it in the direction of increasing the true anomaly, f, and W - axis completes the triad in the positive sense. The relations between the two systems are given from Fig.2, after eliminating the flight path angle φ, between them as:

$$F_R = \frac{(1+e\cos f)}{\sqrt{1+e^2+2e\cos f}}F_T - \frac{(e\sin f)}{\sqrt{1+e^2+2e\cos f}}F_N$$

$$F_S = \frac{(e\sin f)}{\sqrt{1+e^2+2e\cos f}}F_T + \frac{(1+e\cos f)}{\sqrt{1+e^2+2e\cos f}}F_N$$

$$\begin{aligned}
\left(\frac{da}{dt}\right)_D &= -\frac{B_C\rho V_s^2}{n\sqrt{1-e^2}}\sqrt{1+e^2+2e\cos f}\\
\left(\frac{de}{dt}\right)_D &= -\frac{B_C\rho V_s^2\sqrt{1-e^2}}{na}\frac{(e+\cos f)}{\sqrt{1+e^2+2e\cos f}}\\
\left(\frac{d\omega}{dt}\right)_D &= -\frac{B_C\rho V_s^2\sqrt{1-e^2}}{nae}\frac{\sin f}{\sqrt{1+e^2+2e\cos f}}\\
\left(\frac{dM}{dt}\right)_D &= n-\frac{B_C\rho V_s^2}{na}\frac{e\left(1-e^2\right)\sin f}{\sqrt{1+e^2+2e\cos f}}\left(\frac{1}{(1-e^2)+\sqrt{1-e^2}}-\frac{1}{1+e\cos f}\right)
\end{aligned} \tag{6}$$

Where, $B_C = \frac{A}{m}C_D$, called the ballistic coefficient.
We have to express the satellite velocity ${V_s}^2$ in the form:

$$V_s^2 = \frac{\mu}{a(1-e^2)}\left(1+2e\cos f+e^2\right) \tag{7}$$

Substituting Eq. 7 into Eq. 6 we have the variations of the orbital elements due to drag in the form:

$$\left(\frac{da}{dt}\right)_D = -\left(\frac{\mu B_C\rho}{na}\right)\frac{\left(1+2e\cos f+e^2\right)^{3/2}}{(1-e^2)^{3/2}}$$

$$\left(\frac{de}{dt}\right)_D = -\left(\frac{\mu B_C\rho}{na^2}\right)\left(\frac{e+\cos f}{\sqrt{1-e^2}}\right)\sqrt{1+e^2+2e\cos f}$$

$$\left(\frac{d\omega}{dt}\right)_D = -\left(\frac{\mu B_C\rho}{na^2e}\right)\left(\frac{\sin f}{\sqrt{1-e^2}}\sqrt{1+e^2+2e\cos f}\right)$$

$$\left(\frac{dM}{dt}\right)_D = n-\left(\frac{\mu B_C\rho}{na^2e}\right)\left(\frac{e\sin f}{(1-e^2)+\sqrt{1-e^2}}-\frac{1}{1+e\cos f}\right)\sqrt{1+e^2+2e\cos f}$$

Since we shall consider only the secular effects of the drag force on the motion of the satellites, we average Eq. 7 with respect to the true anomaly f, to obtain:

$$\left(\overline{\frac{da}{dt}}\right)_D = -\left(\frac{\mu B_C\rho}{na}\right)\left(1+\frac{3}{4}e^2+\frac{21}{64}e^4\right) \tag{8}$$

$$\left(\overline{\frac{de}{dt}}\right)_D = -\left(\frac{\mu B_C\rho}{na^2}\right)\left(\frac{1}{2}e-\frac{5}{16}e^3\right) \tag{9}$$

$$\left(\frac{\overline{d\omega}}{dt}\right)_D = 0 \ , \quad \left(\frac{\overline{dM}}{dt}\right)_D = n$$

Where the bar indicates that these rates contain secular terms only.

Therefore, the drag cause secular changes only on the semi major axis and the eccentricity of the satellite orbit.

We can now consider the air density ρ in the form [9] as:

$$\rho = \rho_0 \, e^{-(\eta-\eta_0)/H}$$

Where

ρ_o is the air density at perigee,

η is the satellite altitude,

η_o is the altitude at the perigee,

H is the scale height.

With the relation $\mu = n^2 a^3$ we can rewrite Eqs. 8, 9 as

$$\left(\frac{\overline{da}}{dt}\right)_D = -n\,a^2 \left(B_c \, \rho_0 e^{-(\eta-\eta_0)/H}\right) \left(1 + \frac{3}{4}e^2 + \frac{21}{64}e^4\right) \tag{10}$$

$$\left(\frac{\overline{de}}{dt}\right)_D = -n\,a \left(B_c \, \rho_0 e^{-(\eta-\eta_0)/H}\right) \left(\frac{1}{2}e - \frac{5}{16}e^3\right) \tag{11}$$

Integrating Eqs. 10 and 11 with respect to the time t we obtain the secular variation in the semi-major axis and eccentricity due to air drag in the form:

$$\Delta \bar{a}_D = -n\,a^2 \left(B_c \, \rho_0 e^{-(\eta-\eta_0)/H}\right) \left(1 + \frac{3}{4}e^2 + \frac{21}{64}e^4\right) \, t$$

$$\Delta \bar{e}_D = -n\,a \left(B_c \, \rho_0 \, e^{-\,(\eta-\eta_0)/H}\right) \left(\frac{1}{2}e - \frac{5}{16}e^3\right) \, t$$

That represents the secular changes in the orbit due to air drag.

5 Adding Perturbing Forces

We shall consider the effect of perturbation on the orbital elements due to the atmospheric drag. So, We will express the orbital elements of the two satellites in the form:

$$\sigma_j(t) = \sigma_{jo} + (\Delta\sigma_j)_D \qquad j = 1,2.$$

Where $\sigma_j\,(t)$ represent respectively any of the orbital elements, σ_{j0} the unperturbed element, and $(\Delta\sigma_j)_D$denote the perturbations in the elements due to drag force. The expansion of the perturbed visibility function about some epoch time t_0 can be obtained by Taylor expansions about the osculating elements $(a_{0\,j}, e_{0\,j}, i_{0\,j}, \Omega_{0\,j}, \omega_{0\,j}, M_{0\,j})$ up to the first order as:

$$F(a_j, e_j, i_j, \Omega_j, \omega_j, M_j) = U(a_{0j}, e_{0j}, i_{0j}, \Omega_{0j}, \omega_{0j}, M_{0j}) + \sum_{s=1}^{6} \left(\frac{\partial U}{\partial \sigma_s}\right)_0 \Delta\sigma_s \tag{12}$$

The summation ranges from s = 1 to s = 4, where s = 1 , 2 represent the elements (a_1, e_1) and s = 3 , 4 represent (a_2, e_2) respectively.

6 Numerical Examples

In what follows the visibility function were tested for some examples to obtain the mutual visibility between two Earth Satellites. The orbital elements for some satellites were obtained from the Center for Space Standards & Innovation and are listed in Tables 1, 2.

The visibility intervals with the action of air drag are shown in Figures 4, 6, 8 according as the sign of the visibility function given in Eq. (12) and without any perturbing force are shown in Figures 3, 5, 7, and are listed in Table 3, 4 and 5.

Table 1 Norad Two - Line Element Sets For The Satellites AQUA, ARIRANG-2, HST and ODIN

Satellite Orbital Elements	1-AQUA	2-ARIRANG-2	3-HST	4-ODIN
Equivalent altitude (Km)	699.588	682.6205	543.2687	540.5256
a (Km)	7077.725	7060.757	6921.405	6918.662
n (rev/min)	0.010408	0.010445	0.010779	0.010769
e	0.000286	0.001669	0.000256	0.001057
i (degree)	98.2031	98.0676	28.4705	97.591
Ω (degree)	121.6097	76.9906	17.611	200.4958
ω (degree)	54.081	258.4665	301.12	186.4076
M (degree)	125.1605	101.4671	170.9719	173.7019
$\rho\ (kg/km^3)$	3.63E-05	4.6E-05	0.000354	0.000369
$\rho_o\ (kg/km^3)$	0.000145	0.000145	0.000697	0.000697
h_0(Km) (kg/km^3)	600	600	500	500
H (Km)	71.835	71.835	63.822	63.822
Epoch Year & Julian Date	18180. 59770749	18180. 82019665	18182.935593	18182.93790454
time of data (min)	2018 06 29 13:31:30	2018 06 29 19:41:03.004	2018 07 01 21:57:32.134	2018 07 01 22:30:32.994
B^*	2.5E-05	3.76E-05	1.36E-05	5.61E-05
$BC = C_D A/m\ (m^2/kg)$	5.4E-05	8.1E-05	6.11E-06	2.52E-05

7 Conclusions

We referred to the first column (The Function of Visibility without any perturbation) in Ammar and Hassan [1] of this paper, now we refer to the second column (The Function of Visibility with the Air Drag Force)

In the Table 3 (Visibility Intervals Between AQUA and ARIRANG2), In the second column (with the Air Drag Force), the increase and decrease in oscillation is noticeable, the time of large periods increases and the time of the small periods decreases gradually, then the effect of the air drag force appears clearly.

Table 2 Norad Two - Line Element Sets For The Satellites CFESAT and MTI

Satellite Orbital Elements	5-CFESAT	6-MTI
Equivalent altitude (Km)	468.8831	412.5092
a (Km)	6847.02	6790.646
n (rev/min)	0.010953	0.011074
e	0.000582	0.000812
i (degree)	35.4247	97.5789
Ω (degree)	203.043	17.7612
ω (degree)	183.8662	345.6071
M (degree)	176.2019	143.5229
ρ (kg/km^3)	0.001162	0.003008
ρ_o (kg/km^3)	0.001585	0.003725
h_0(Km) (kg/km^3)	450	400
H (Km)	60.828	58.515
Epoch Year & Julian Date	18182.5017322	18182.7746284
time of data (min)	2018 07 01 12:02:28.526	2018 07 01 18:02:08.608
B^*	6.71E-05	4.84E-05
$BC = C_D A/m$ (m^2/kg)	1.33E-05	4.07E-06

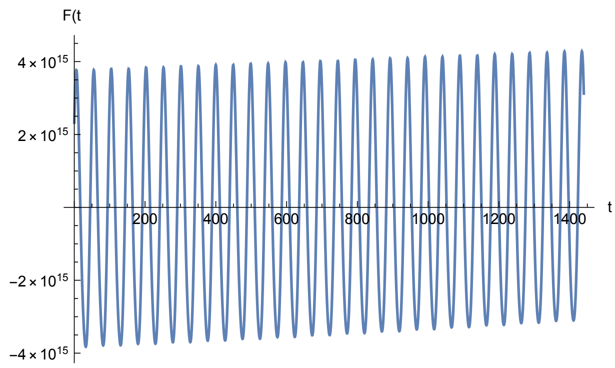

Fig. 3 Visibility Intervals Between AQUA and ARIRANG2 during 24-H

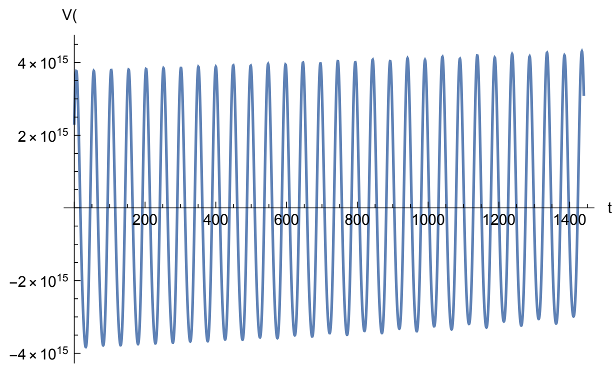

Fig. 4 Visibility Intervals Between AQUA and ARIRANG2 24-H with Air Drag Force

Table 3 Visibility Intervals Between AQUA And ARIRANG2 During 24 Houres

	Without Air Drag Force				With Air Drag Force			
	Rise	Set	visibility time m	s	Rise	Set	visibility time m	s
1	17.1074	44.8663	27	45.534	17.1027	44.8676	27	45.894
2	66.4086	94.0482	27	38.376	66.4145	94.0542	27	38.382
3	115.669	143.318	27	38.94	115.674	143.306	27	37.92
4	164.973	192.499	27	31.56	164.973	192.519	27	32.76
5	214.236	241.768	27	31.92	214.25	241.742	27	29.52
6	263.542	290.948	27	24.36	263.536	290.982	27	26.76
7	312.807	340.216	27	24.54	312.83	340.177	27	20.82
8	362.115	389.396	27	16.86	362.103	389.443	27	20.4
9	411.382	438.663	27	16.86	411.416	438.61	27	11.64
10	460.692	487.842	27	8.94	460.675	487.903	27	13.68
11	509.962	537.108	27	8.76	510.006	537.041	27	2.1
12	559.276	586.286	27	6	559.251	586.362	27	6.66
13	608.547	635.552	27	0.3	608.6	635.472	26	52.32
14	657.863	684.729	26	51.96	657.831	684.819	26	59.28
15	707.135	733.994	26	51.54	707.199	733.9	26	42.06
16	756.453	783.171	26	43.08	756.416	783.275	26	51.54
17	805.728	832.435	26	42.42	805.802	832.327	26	31.5
18	855.048	881.611	26	33.78	855.004	881.729	26	43.5
19	904.325	930.874	26	32.94	904.41	930.753	26	20.58
20	953.647	980.049	26	24.12	953.597	980.182	26	35.1
21	1002.93	1029.31	26	22.8	1003.02	1029.18	26	9.6
22	1052.25	1078.49	26	14.4	1052.19	1078.63	26	26.4
23	1101.35	1127.75	26	13.2	1101.64	1127.6	25	57.6
24	1150.86	1176.92	26	3.6	1150.79	1177.08	26	17.4
25	1200.14	1226.18	26	2.4	1200.26	1226.02	25	45.6
26	1249.47	1275.36	25	53.4	1249.4	1275.53	26	7.8
27	1298.75	1324.62	25	52.2	1298.88	1324.44	25	33.6
28	1348.08	1373.79	25	42.6	1348.01	1373.89	25	58.2
29	1397.37	1423.05	25	40.8	1397.5	1422.68	25	21

In the Table 4 (Visibility Intervals Between HST and ODIN), In the second column (with the Air Drag Force), the increase and decrease in oscillation is noticeable, the time of large periods increases and the time of the small periods decreases gradually, then the effect of the air drag force appears clearly.

In Table 5 (Visibility Intervals Between CFESAT and MTI), In the second column (with the Air Drag Force), the increase in oscillation is noticeable and greater than the previous examples, because the semi-major axis is smaller than the other one in the previous examples and less than 600 Km, then the effect of the air drag force appears clearly. It is also noticed that there is a low number of periods of visibility function that affects the air Drag force.

The secular variations of the orbital elements due the Effect of the Air Drag Force was considered and it

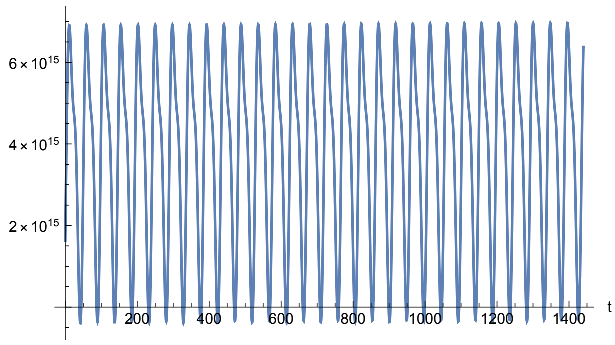

Fig. 5 Visibility Intervals Between HST and ODIN For 24-H

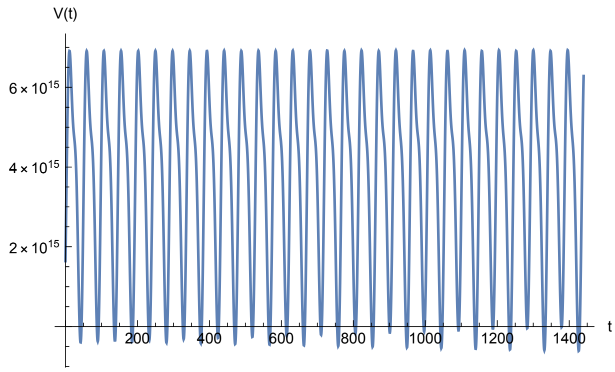

Fig. 6 Visibility Intervals Between HST and ODIN For 24-H with Air Drag Force

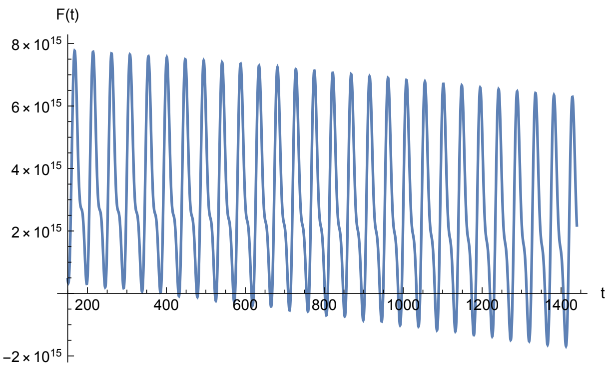

Fig. 7 Visibility Intervals Between CFESAT and MTI For 24-H

appeared obviously in the previous tables. The new method exploits sophisticated analytic models of the orbit and therefore provides direct computation of rise-set times. Numerical examples for some satellites were given to chick the validity of the method.

Table 4 Visibility Intervals Between HST and ODIN 24 Houres

	Without Air Drag Force				With Air Drag Force			
	Rise	Set	visibility time		Rise	Set	visibility time	
			m	s			m	s
1	39.3255	44.4432	5	7.062	39.3208	44.4432	5	7.344
2	87.2035	92.0758	4	52.338	87.168	92.1059	4	56.274
3	134.82	139.913	5	5.52	134.901	139.846	4	56.7
4	182.699	187.545	4	50.76	182.584	187.635	5	3.06
5	230.316	235.383	5	4.02	230.484	235.246	4	45.72
6	278.195	283.014	4	49.14	278.002	283.163	5	9.66
7	325.812	330.852	5	2.4	326.072	330.642	4	34.2
8	373.691	378.843	5	9.12	373.42	378.69	5	16.26
9	421.307	426.322	5	0.9	421.663	426.033	4	22.2
10	469.188	473.952	4	45.84	468.84	474.217	5	22.62
11	516.803	521.792	4	59.34	517.259	521.42	4	9.66
12	564.684	569.421	4	44.22	564.261	569.743	5	28.92
13	612.298	617.261	4	57.72	612.861	616.8	3	56.34
14	660.18	664.98	4	48	659.682	665.267	5	35.1
15	707.794	712.731	4	56.22	708.47	712.175	3	42.3
16	755.676	760.359	4	40.98	755.105	760.791	5	41.16
17	803.289	808.201	4	54.72	804.087	807.541	3	27.24
18	851.172	855.828	4	39.18	850.528	856.314	5	47.16
19	898.785	903.67	4	53.1	899.714	902.896	3	10.92
20	964.668	951.297	4	37.74	945.952	951.836	5	53.04
21	994.28	999.14	4	51.6	995.353	998.24	2	53.22
22	1042.16	1046.77	4	36.6	1041.38	1047.36	5	31.8
23	1089.78	1094.61	4	49.8	1091.01	1093.57	2	33.6
24	1137.66	1142.23	4	34.2	1136.8	1142.88	6	4.8
25	1185.27	1190.08	4	48.6	1186.69	1188.87	2	10.8
26	1233.16	1237.7	4	32.4	1232.23	1238.4	6	10.2
27	1280.77	1285.55	4	46.8	1282.42	1284.12	1	42
28	1328.65	1333.17	4	31.2	1327.66	1333.92	6	15.6
29	1376.26	1381.02	4	45.6	1378.23	1379.29	1	3.6
30	1424.15	1428.64	4	29.4	1423.08	1429.44	6	21.6

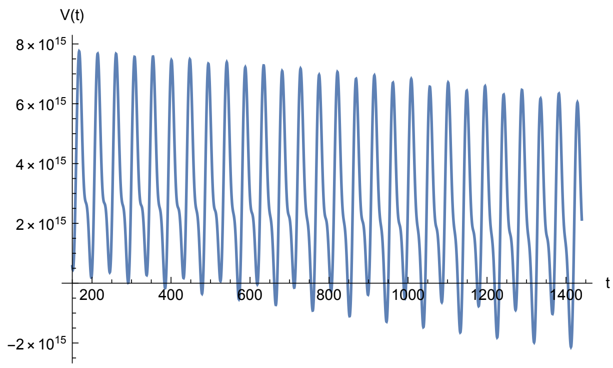

Fig. 8 Visibility Intervals Between CFESAT and MTI For 24-H Air Drag Force

Table 5 Visibility Intervals Between CFESAT and MTI 24 Houres

	Without Air Drag Force				With Air Drag Force			
	Rise	Set	visibility time		Rise	Set	visibility time	
			m	s			m	s
1	430.519	432.975	2	27.36	383.281	386.757	3	28.56
2	476.988	479.867	2	52.74	475.837	480.888	5	3.06
3	523.051	527.147	4	5.76	568.562	574.83	6	16.08
4	569.583	573.973	4	23.4	617.63	619.378	1	44.88
5	615.801	621.095	5	17.64	661.372	668.709	7	20.22
6	662.353	667.899	5	32.76	710.16	713.559	3	23.94
7	708.642	714.947	6	18.3	754.234	762.517	8	16.98
8	755.203	761.74	6	32.22	802.941	807.477	4	32.22
9	801.535	808.742	7	12.42	847.133	856.283	9	9
10	848.101	855.526	7	25.5	895.808	901.304	5	29.76
11	894.462	902.496	8	2.04	940.061	950.015	9	57.24
12	941.03	949.275	8	14.7	988.72	995.079	6	21.54
13	987.413	996.22	8	48.42	1033.01	1043.72	10	42.6
14	1033.98	1042.99	9	0.6	1081.66	1088.82	7	9.6
15	1080.38	1089.92	9	32.4	1125.98	1137.4	11	25.2
16	1126.95	1136.69	9	44.4	1174.61	1182.52	7	54.6
17	1173.37	1183..6	10	13.8	1218.97	1231.06	12	5.4
18	1219.93	1230.37	10	26.4	1267.58	1276.23	8	39
19	1266.36	1277.26	10	54	1311.98	1324.69	12	42.6
20	1312.93	1324.02	11	5.4	1360.55	1369.91	9	21.6
21	13.5937	1370.9	11	31.8	1405	1418.31	13	18.6
22	1405.93	1417.66	11	43.8	-	-	-	-

References

[1] M. K. Ammar, M. R. Amin, M.H.M. Hassan, (2018) "Visibility Intervals between Two Artificial Satellites Under the action of Earth Oblateness", "Applied Mathematics and Nonlinear Sciences", Acceptted.

[2] Escobal,P.R.(1963) "Rise and set Times of a Satellite about an Oblate Planet," AIAA Journal Vol. I, No. 10, October, pp. 2306-2310.

[3] Escobal,P.R.(1965), "Methods of orbit determination, Robert E. Krieger Publishing Company, Huntington, New York, pp. 26-29 and 360 - 369.

[4] Lawton, J. A.(1987), "Numerical Method for Rapidly Determining Satellite - Satellite and Satellite-Ground Station In - View Periods, " Journal of guidance, Navigation, and Control, vol. 10, January-February, pp. 32-36.

[5] Salvatore Alfano , David Negron, Jr., and Jennifer L. Moore (1992), "Rapid Determination of Satellite Visibility Periods", The Journal of the Astronautical Sciences, Vol.40, No.2, April-June, pp.281-296.

[6] P. L. Palmer & Yan Mai "A Fast Prediction Algorithm of Satellite Passes", 14th Annual AIAA/USU Conference on Small Satellite, Surrey Space Centre University of Surrey, Guildford,GU2 7XH, UK]

[7] Brouwer, D. and Clemence, G. M.: (1961), Methods of Celestial Mechanics, Academic Press, New York.

[8] Vallado, D.A.:(2001) "Fundamentals of Astrodynamics and. Applications", 2nd. edition, Microcosm . press, Kluwer Academic publishers,

[9] A.E. Roy, (2005), "Orbital Motion" 4th. Intitute Of Physics Publishing Bristol And Philadelphia.